JOURNAL OF MATERIALS SCIENCE 21 (1986) 1145–1150

Temperature and porosity effects on the fracture of fine grain size MgO

R. BADDI, J. CRAMPON, R. DUCLOS
Laboratoire de Structure et Propriétés de l'Etat Solide, UA CNRS 234, Université de Lille I, 59655 Villeneuve d'Ascq Cédex, France

The strength of three fine grain size magnesias (< 0.8 μm) has been studied as a function of porosity and temperature from 20 to 1200° C. In the low-temperature region ($T \leqslant 800°$ C) fracture occurs by the extension of flaws introduced during the specimen machining. In this case the fracture stress can be related to porosity by an exponential law. In the high-temperature region ($T > 800°$ C) plasticity increases the size of pre-existing flaws, but this effect is partially annihilated by a rapid increase with temperature in the effective surface energy for fracture initiation. This entails only a slow decrease in fracture stress with temperature. These results are correlated with observations of fracture surfaces by scanning and transmission electron microscopy.

1. Introduction

During the last ten years several studies which concern the plasticity of ceramic materials have shown that contrary to coarse grain ceramics, fine grain materials (with a grain size less than a few micrometres) [1–3] can be deformed without rupture to very considerable strains, up to 100%; it was then pointed out that under optimized conditions (grain size, temperature, strain rate), superplasticity was possible in ceramics.

In addition to the small grain size, the superplastic behaviour is generally associated in these materials with a weak porosity, even in dense materials, located at triple points, which favours the grain intercalation mechanism [4] and thus prevents specimen microcracking [5].

However, in spite of these results, relatively little is known about the fracture mechanisms of such fine grain ceramics, whilst in coarse grain ceramics fracture experiments have been widely reported [6–8]. In particular, what is the influence of the fine grain size on fracture in the temperature range where a superplastic behaviour is observed?

With this object, the brittle fracture mechanisms of ultra fine grain magnesias (0.2 to 1 μm) have been studied between room temperature and 1200° C. The results which are presented in this paper, the first on such fine grain materials, consist primarily in the determination of the effective surface energy for fracture initiation, and the discussion of fracture mechanisms in relation to observations of fracture zones by scanning electron microscopy (SEM) or transmission electron microscopy (TEM).

TABLE I Microstructural parameters of as-sintered magnesias

Material	Sintering pressure (MPa)	Density (% of theoretical)	Mean grain size (μm)
A	40	80 ± 1	0.1
B	50	87 ± 1	0.2
C	60	93 ± 1	0.5

So this work is not only an extension of previous work on MgO by Evans *et al.* [7] to submicrometre grain sizes, but is also a study in a grain size range where dislocation influence is very limited.

2. Experimental procedure

2.1. Magnesia fabrication

Three kinds of magnesia have been used in this study. They have been obtained as discs of polycrystalline MgO (30 mm in diameter by 6 mm thick) by a reactive hot-pressing technique of magnesium hydroxide powder [9]. The powder is heated in a graphite die up to 900° C under a pressure from 40 to 60 MPa. This technique has allowed us to obtain relatively dense fine grain polycrystals without doping elements; it uses the high reactivity of the powder at the decomposition temperature of the hydroxide (about 450° C), and the low sintering temperature then helps us to retain the small grain size.

Density and grain size of the as-sintered discs are dependent on the sintering pressure. Typical results are given in Table I. The mean grain size was determined by a linear intercept method on photomicrographs obtained by TEM. The detailed procedure of the preparation method is described elsewhere [10].

2.2. Mechanical testing

The fracture stresses and effective surface energy values, γ_i, were determined by three-point bend tests with a knife-edge span of 20 mm [10]. The tests up to 1200° C were conducted in an SiC furnace in air, the alumina device being mounted on an Instron testing machine. The mobile crosshead was displaced at 0.2 mm min^{-1} ($\dot{\varepsilon} \simeq 2 \times 10^{-4}$ sec^{-1}) for fracture stress measurements and 0.5 mm min^{-1} for γ_i measurements in order to prevent macroscopic plastic deformation of specimens at the highest test temperatures.

0022–2461/86 $03.00 + .12

TABLE II Microstructural parameters after annealing at 1200° C

Material	Density (% of theoretical)	Average grain size (μm)
A	82	0.3
B	88	0.5
C	93	0.7

2.3. Sample preparation

Specimens needed for three-point bend experiments were diamond-sawn from the discs into bars of approximative dimensions 25 mm × 4 mm × 4 mm. To avoid an excessive grain growth during high-temperature tests, all the samples were annealed for 75 min at 1200° C before tests. The new microstructural parameters are given in Table II.

The microstructure at this stage consisted of equiaxed grains with porosity located at triple points (Fig. 1). Moreover, we did not observe a second phase at grain boundaries. The different faces of sample were then mechanically polished. Chemical polishing was not used.

In specimens needed for γ_i measurements a notch of 1 mm depth was introduced with a diamond saw in the centre section; SEM observations showed that sharp cracks were introduced during this machining along the notch root. The γ_i values were then calculated by the relation

$$\gamma_i = Y^2 \frac{\sigma_f^2 a}{2E} \quad (1)$$

where σ_f is the fracture stress for the notch depth a, E the Young's modulus measured as a function of temperature and Y a form factor equal to 1.80 in our case (see Brown and Srawley [11]).

2.4. Microscopic examination

Fracture surfaces were examined after tests by SEM. To this end a thin gold film was deposited on fracture faces by evaporation. In addition to SEM observations, thin foils, cut parallel to fracture faces and thinned by ionic bombardment, were also observed by TEM at 100 kV. This allows us a better understanding of fracture mechanisms, in particular the role of plasticity near the crack tip.

Figure 1 Typical microstructure of Material B; TEM micrograph. Scale bar = 1 μm.

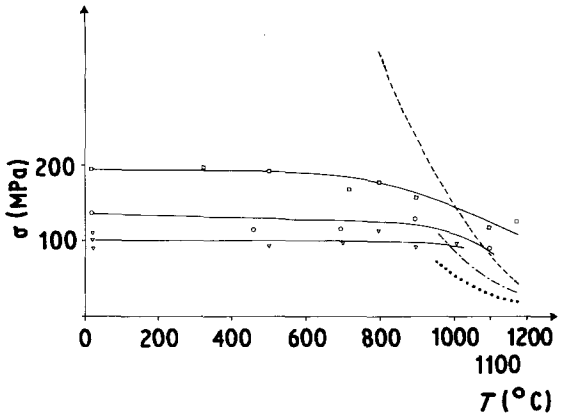

Figure 2 Variation of the fracture stress with temperature for materials A (▽), B (○), and C (□). The yield stress σ_{ys} is also shown: (· · ·) Material A, (–·–) Material B, (– – –) Material C.

3. Results

3.1. Bend strength

The fracture stresses for the three magnesias A, B and C are shown in Fig. 2 as a function of temperature. For all tests, fracture was always brittle, characterized by a linear load–deflexion curve except for Materials A and B at the highest test temperature, where a very weak deviation from linearity was observed on the $P - \delta$ curves just before fracture. In Fig. 2 the yield stress σ_{ys} measured in compression at a strain rate of 1.8×10^{-4} sec^{-1} is also reported for the highest temperatures. In this temperature region and for each magnesia, the yield stress is similar to the fracture stress.

For Materials B and C the fracture stress is temperature-independent up to 800° C and then slightly decreases with temperature, while for the most porous magnesia (Sample A) the rupture stress is relatively constant, about 100 MPa, over the whole experimental temperature range.

From room temperature to 800° C the variation of fracture stress with porosity can be fitted to a relationship of the form

$$\sigma_f = \sigma_0 \exp(-bp) \quad (2)$$

where σ_0 is the fracture stress at zero porosity and p the porosity fraction. In our case, values of σ_0 and b are $\sigma_0 = 300$ MPa and $b = 2.3$. This value of bend strength at zero porosity is equal to that reported by Vasilos *et al.* [12] in the case of a dense hot-pressed magnesia of average grain size 3 μm. In the same way, at equivalent porosity, the bend strengths of our magnesias are at least equal to those measured by Evans *et al.* [7] for their materials.

3.2. The effective surface energy for fracture initiation

The γ_i values obtained from tests on notched specimens are presented in Fig. 3 as a function of tempera-

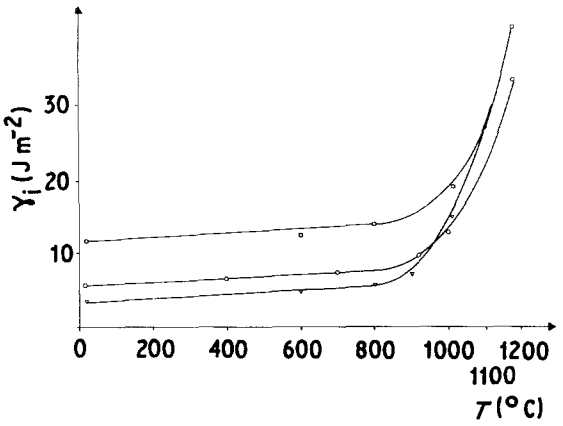

Figure 3 Variation of γ_i with temperature for the Materials A (▽), B (○) and C (□).

ture. For the three tested magnesias, the surface energy γ_i slightly increases with temperature up to 800° C, varying from 11.5 J m^{-2} at room temperature to 14 J m^{-2} at 800° C for the most dense material, and from 3.5 J m^{-2} at 20° C to 5.5 J m^{-2} at 800° C for the most porous one.

In this temperature range γ_i can be related to porosity by an expression of the form

$$\gamma_i = \gamma_{i0} \exp(-cp) \quad (3)$$

with $\gamma_{i0} = 24$ J m^{-2} and $c = 11$. This value of c is in agreement with the literature [13] for intergranular fracture with pores smaller than the grain size, the present fracture mode.

For temperatures higher than 800° C the effective surface energy γ_i rapidly increases to reach a value of about 35 to 40 J m^{-2} at 1150° C; the γ_i values are then relatively independent of porosity in this temperature range.

3.3. The flaw size

The largest flaws we have observed in our materials arise from specimen preparation: machining introduces surface flaws, the typical size of which is about 10 μm (Fig. 4).

Though the cracks which are shown in Fig. 4 are not straight and narrow like those generally introduced during mechanical polishing, they are really due to the machining process. The origin resides in the microstructure of our samples, the grain size of which is generally lower than that of the abrasives used for polishing and cutting. These then pull out grain packets from surfaces during machining and induce the microcracks of variable orientation which are observed. If these microcracks were intrinsic to the processing technique they would be visible on the fracture surfaces, at least for samples fractured at room temperature, which is not the case. In the same way, the size of intrinsic cracks ought to depend on the stress applied during hot pressing; this is contrary to our observations. These various arguments are therefore in favour of extrinsic cracks, i.e. cracks introduced after processing during cutting and polishing.

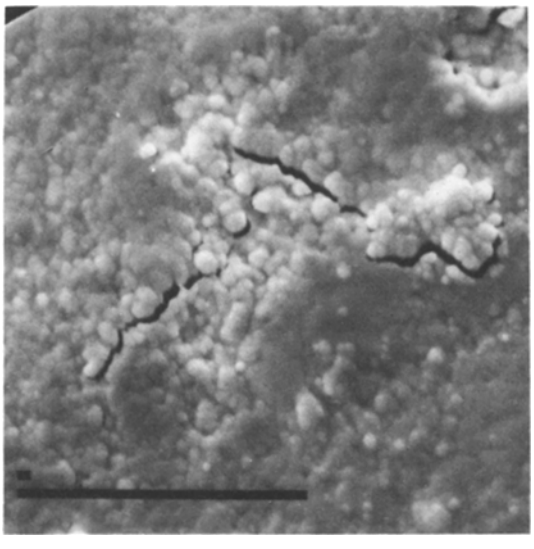

Figure 4 Surface flaw introduced during sample machining. Scale bar = 10 μm.

In the bulk of the specimen, TEM only reveals an intergranular porosity: the size of the largest pores, the major defects, is about one micrometre. We have not observed by this method large cracks like those of Fig. 4. In fact these cracks introduced during the preparation of thin foils disappear during the ionic thinning, a thickness of about 20 μm being removed from each face, and are consequently invisible by this technique. This remark is important for future TEM observations, because it means that the microcracks observed afterwards are due to fracture mechanisms.

3.4. Fracture mode examination

Whatever the temperature and porosity, the fracture surfaces of all the specimens are macroscopically flat and fracture is fully intergranular; this originates in the fine grain size and porosity of our samples.

Figs. 5a and b present two scanning micrographs of Materials A and C fractured at room temperature. These observations are similar to those which can be made up to 800° C. Some small and shallow microcracks are observed.

At high temperature ($T > 800$° C) the situation is very different from the previous one, as Figs. 6 and 7 show. These represent micrographs of Materials A and C, respectively, fractured at 1100 and 1180° C. Numerous microcracks, the length of which can reach 10 μm and the depth about ten grains, are clearly visible. In addition to these observations, Fig. 8 shows that in secondary microcracks the grain surface is undulating. These undulations have been also observed by TEM inside thin foils cut in the vicinity of fracture surfaces. They are observed whatever the porosity fraction in this temperature range (Fig. 9).

4. Discussion

The different curves and surface observations which have been presented show a transition at 800° C; the discussion will be therefore separated in two parts.

4.1. Low-temperature range $T \leqslant 800$° C

In this temperature range fracture occurs by intergranular separation. The measured energies for fracture initiation γ_i are in excess of the theoretical thermodynamic surface energy, which is less than 1 J m^{-2}. As a first explanation the fracture surface is not

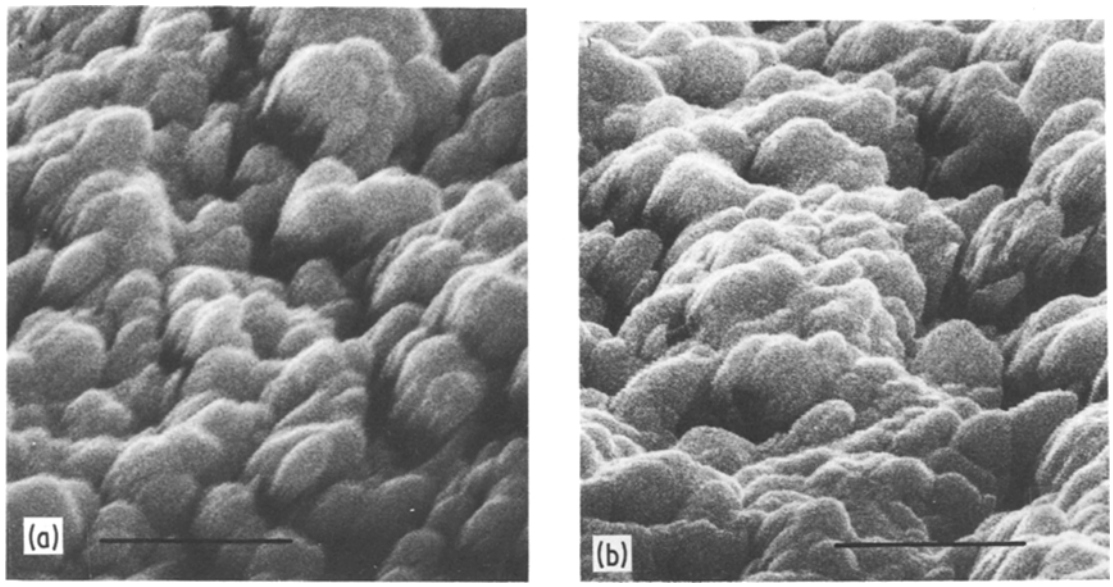

Figure 5 SEM micrographs of fracture surfaces at room temperature. Scale bar = 1 μm. (a) Material A, (b) Material C.

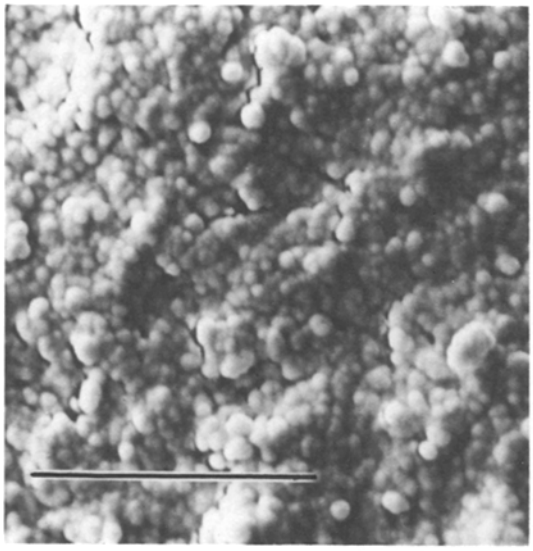

Figure 6 SEM micrograph of fracture surface of Material A; T = 1100° C. Scale bar = 10 μm.

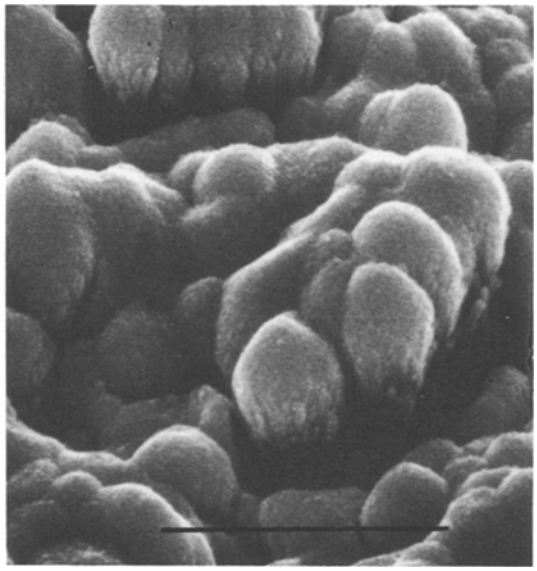

Figure 8 SEM micrograph of fracture surface showing ripples at the grain bases of secondary microcracks (Material C fractured at 1180° C). Scale bar = 2 μm.

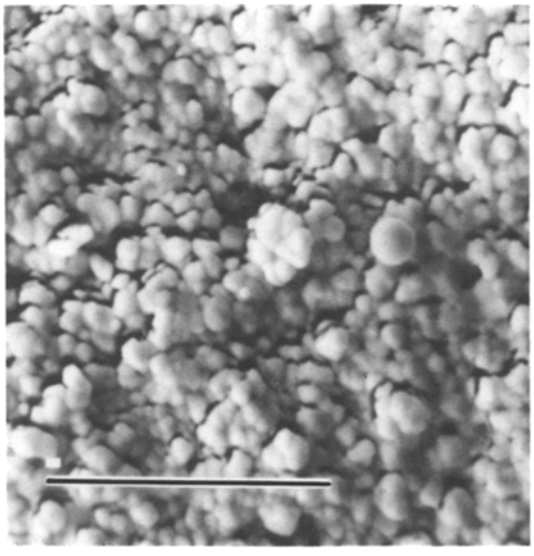

Figure 7 SEM micrograph of fracture surface of Material C; T = 1180° C. Scale bar = 10 μm.

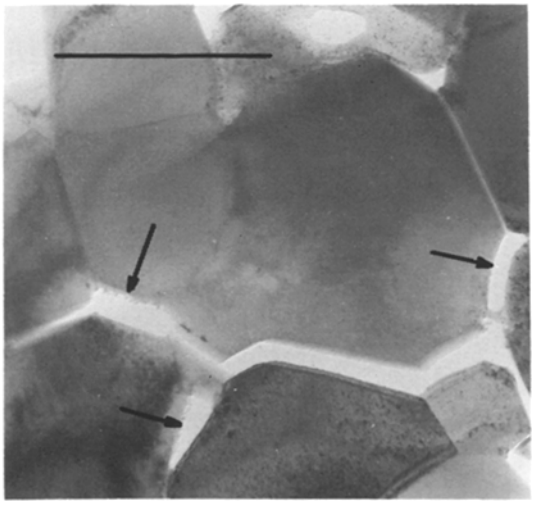

Figure 9 TEM micrograph of Material C fractured at 1180° C showing microcracks and ripples (arrows). Scale bar = 0.5 μm.

flat on a microscopic scale, but this cannot explain entirely the differences in energy, in particular for the densest magnesia. In fact the greater part of the difference originates from the plasticity, or more exactly from the non-reversible deformation localized in the vicinity of the crack front as grain-boundary sliding, which induces microcracking in the absence of accommodation by surface diffusion. This process requires energy and consequently increases the effective surface energy for fracture initiation.

The influence of grain size, which slightly increases with density, is probably negligible in our case in so far as

(i) fracture is intergranular, and
(ii) dislocations, which are almost always absent from our fine grain materials (in contrast to coarse grain ones), cannot largely contribute to plasticity.

On the contrary, the influence of porosity is important. As previously discussed by Evans *et al.* [7] and other authors, pores at grain boundaries generally have sharp angles, which on the one hand do not stop the crack, but on the other hand reduce the surface fractured by the propagation crack; whereas transgranular pores, generally spherically shaped, blunt the crack along its length.

Our materials contain only an intergranular porosity, which can be either open or closed. Thus the open porosity acts as in the first case in reducing the area of fractured surface, while the closed pores, containing gases which occur from the processing technique, are generaly more spherical than the open pores and can thus have a tendancy to blunt the crack.

In the investigated porosity range, open and closed porosities vary in the opposite way with density. So the conjugate effects of the two kinds of porosity are in agreement with observations, i.e. the increase in surface energy with density.

The critical flaw size has been calculated by considering an elliptical shape of defect; one obtains a size of about 10 μm whatever the density. This size is about identical with that of machining defects, the bend strength of our materials is thus controlled by an extrinsic defect introduced during machining, and in this way the independence of the flaw size with density and temperature, in this temperature range, can be understood.

4.2. High-temperature range $T > 800^\circ$ C

In this temperature range, fracture still occurs by intergranular separation and one observes a rapid increase in the effective surface energy γ_i with temperature.

800° C is the lowest temperature above which diffusion of matter is sufficiently fast to have an important effect in plasticity mechanisms of our fine grain materials [2]. The increase in γ_i can then be related to plastic deformation processes in a region ahead of the crack front, the size of which varies from a few micrometres to some tens of micrometres according to the temperature and porosity. The role of dislocations in plasticity is very limited in these fine grain materials. This is firstly because grains are generally free of

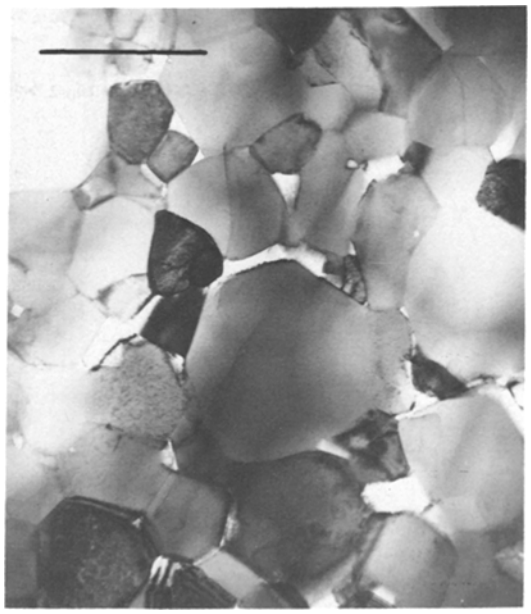

Figure 10 TEM micrograph of Material C fractured at 1180° C showing grains free of dislocations. Scale bar = 1 μm.

dislocations, as shown by TEM observations on thin foils obtained in regions near the fracture face (Fig. 10). In this figure, some undulating contrast inside the grains can arise from grain superpositions in the thickness of the foil, due to their small size. Secondly, rheological equations show that, in this grain size range, deformation by surface or grain-boundary diffusion is more efficient than a dislocation plasticity [2].

In this temperature range, grain-boundary sliding must be very active. At first, surface and grain-boundary diffusion succeeds in accommodating boundary sliding and in relaxing stress concentrations. This involves an increase in applied stress in order to continue the deformation test at the same rate. However, as stress increases, grain-boundary sliding becomes faster and faster and accommodation by diffusion is more and more difficult; this then results in numerous microcracks like the ones observed in Figs. 6 and 7. Some of the secondary microcracks may have been produced by a diffusive porosity flow in order to locally accommodate the stress distribution [14]. The undulations which are observed on the grain surface near secondary microcracks, in this temperature range, can under these conditions be a sign of the diffusive opening of microcracks, more especially as such undulating ledges are absent in the low-temperature range.

All these mechanisms contribute to increase greatly the effective surface energy for fracture initiation. The temperature dependence of γ_i can be related to the increase in size of the plastic zone with temperature, in harmony with the decrease in yield stress of the materials.

The plasticity mechanisms, surface and boundary diffusion, which are at the origin of the increase in surface energy for fracture initiation will allow, for strain rates lower than those used in this work, to accommodate stress concentrations and to prevent microcracking at the outset. Very large strains can be then obtained and consequently a superplastic behaviour can be observed.

The weak porosity dependence of γ_i at high temperature in our materials can be due to several competing effects on the overall energy expenditure associated with the fracture. An increase in γ_i with porosity can be related to an increase in the size of the plastic zone ahead of crack; on the other hand stress concentration relaxation by surface and grain-boundary diffusion is easier in more porous magnesias, in so far as the grain size is finer than in denser ones and thus diffusion paths are shorter. These two effects counterbalance the negative effects of porosity which have been already discussed at low temperature, and this leads to an effective surface energy which is nearly independent of porosity.

This result supports the point of view expressed by Crampon [14] according to which the elimination of the residual porosity is not of prime importance for obtaining a superplastic deformation in fine grain MgO.

In this temperature region, the flaw size was calculated as in Section 4.1. It varies from 15 to 50 μm, increasing with temperature and porosity. As specimen machining is the same as previously, the increase in flaw size arises from microcrack opening in the plastic zone. These microcracks link up with the main crack and increase its size. Catastrophic fracture then occurs at lower stresses than those measured in the low-temperature region, the flaw size effect being more important than the increase in effective surface energy. The increase in flaw size was calculated by considering the plane strain zone correction term $K_{Ic}^2/6\pi\sigma_{ys}^2$ [15]. This is listed in Table III. The agreement between experimental and calculated values is good.

TABLE III Values of plastic zone size $K_{Ic}^2/6\pi\sigma_{ys}^2$ (μm)

Material	Temperature (° C)			
	900	1000	1100	1180
A	1	6	40	–
B	–	2	11	35
C	–	2	8	17

5. Conclusions

The fracture of fine grain magnesias can be separated into two temperature regions:

1. At low temperature ($T \leqslant 800°$ C) fracture occurs by the propagation of machining defects. This entails bend strengths and effective surface energies for fracture initiation that are nearly independent of temperature, but dependent on porosity according to exponential laws. In this temperature region, for equivalent porosities, the fracture stress of our materials is similar to or higher than that measured for coarse grain magnesias [7]. However, for the most porous materials, coarse grain magnesias have γ_i values higher than those measured on fine grain magnesias. This shows that dislocations, which are generally present in coarse grain materials, allow by their motion a reduction of stress concentrations at the crack tip, and consequently an increase in γ_i.

2. At high temperature ($T > 800°$) fracture occurs after a preliminary extension of pre-existing defects, due to a plasticity located in the vicinity of the crack front. Nevertheless, the fracture stress is only slowly decreasing. This originates from the rapid increase in effective surface energy γ_i with temperature; γ_i becomes equally independent of porosity. The increase in γ_i comes from stress concentration relaxation by surface diffusion, a more efficient mechanism in our fine grain magnesias than dislocation plasticity in coarse grain ones [7] in this temperature region.

Acknowledgements

The authors wish to thank CNRS for financial support of this work (Contract ATP No. 9 81 13).

References

1. T. E. CHUNG and T. J. DAVIES, *Acta Metall.* **27** (1979) 627.
2. J. CRAMPON and B. ESCAIG, *J. Amer. Ceram. Soc.* **63** (1980) 680.
3. C. CARRY and A. MOCELLIN, *Proc. Brit. Ceram. Soc.* **33** (1983) 101.
4. M. F. ASHBY and R. A. VERRALL, *Acta Metall.* **21** (1973) 149.
5. T. E. CHUNG and T. J. DAVIES, *J. Nucl. Mater.* **79** (1979) 143.
6. A. G. EVANS and R. W. DAVIDGE, *ibid.* **33** (1969) 249.
7. A. G. EVANS, D. GILLING and R. W. DAVIDGE, *J. Mater. Sci.* **5** (1970) 187.
8. R. W. DAVIDGE and G. TAPPIN, *Proc. Brit. Ceram. Soc.* **15** (1970) 47.
9. A. C. D. CHAKLADER, *Nature* **24** (1965) 392.
10. R. BADDI, Thèse de 3è Cycle, Université de Lille I (1984).
11. W. F. BROWN and J. E. SRAWLEY, ASTM STP 410 (American Society for Testing and Materials, Philadelphia, 1966) p. 13.
12. T. VASILOS, J. B. MITCHELL and R. M. SPRIGGS, *J. Amer. Ceram. Soc.* **47** (1964) 606.
13. P. L. PRATT, *Metal Sci.* **14** (1980) 363.
14. J. CRAMPON, in Proceedings of 2nd Risø International Symposium on Metallurgy and Materials Science, Roskilde, September 1983, edited by N. Hansen, A. Horsewell, T. Leffers and H. Lilholt, p. 247.
15. G. R. IRWIN, *Appl. Mater. Res.* **3** (1964) 65.

Received 12 December 1984
and accepted 31 May 1985